Band Structure for Fourteen Semiconductors

Bashar Karaja
Universite de Bourgogne

THE INTRODUCTION In this paper, we embark on a comprehensive exploration of the band structures inherent in 14 semiconductors: AISb, CdTe, GaAs, GaP, GaSb, Ge, InAs, InP, InSb, Si, Sn, ZnS, ZnSe, and ZnTe. Our focus is on the computational recreation of their band structures, specifically honing in on the face-centered cubic (fcc) structures. Employing the potent and efficient tool of empirical pseudopotentials, renowned in the realm of crystalline solid-state physics, we aim to unravel the intricate electronic states within these semiconductors. A mapping of Brillouin zone paths using this method is integral to our approach, ensuring a thorough exploration that paves the way for a detailed computation and analysis of their respective band structures. This study not only contributes to the understanding of semiconductor behavior but also underscores the significance of empirical pseudopotentials as a robust computational tool in unraveling the complexities of crystalline materials.

Methods

In the initial stages of the computational process, the foundation is laid with the definition of unit vectors within reciprocal space. This crucial step is instrumental in constructing the reciprocal lattice vector G, a fundamental component in the analysis of crystalline structures. The qpath, acquired from the BZpath file, plays a pivotal role in guiding the subsequent steps of the process. It serves as a valuable tool in the assembly of the reciprocal lattice. Moving forward, we need to determine the potential V for each semiconductor. This intricate task involves an expansion of V with respect to the reciprocal lattice vectors G, as follows:

$$V_G = V^S_{|G|^2} Cos(G.s) + iV^A_{|G|^2} Sin(G.s) \quad (1)$$

The calculation of form factors relies on Table 1 from Cohen and Bergstresser's 1966[1] study. Due to the dataset's origin in 1966, there is a possibility of incomplete refinement, resulting in minor misalignments in the band structures. Notably, the original dataset omits V0. Consequently, after determining energy levels for each material, the maximum value of the third band is scaled to the Rydberg scale, based on the information provided in Table 1:

Material	V0	VS3	VS8	VS11	VA3	VA4	VA11
Si	-0.7724	-0.21	0.04	0.08	0	0	0
Ge	-0.6951	-0.23	0.01	0.06	0	0	0
Sn	-0.5015	-0.2	0	0.04	0	0	0
GaP	-0.6775	-0.22	0.03	0.07	0.12	0.07	0.02
GaAs	-0.6527	-0.23	0.01	0.06	0.07	0.05	0.01
AlSb	-0.5107	-0.21	0.02	0.06	0.06	0.04	0.02
InP	-0.5627	-0.23	0.01	0.06	0.07	0.05	0.01
GaSb	-0.5112	-0.22	0	0.05	0.06	0.05	0.01
InAs	-0.5251	-0.22	0	0.05	0.08	0.05	0.03
InSb	-0.4460	-0.2	0	0.04	0.06	0.05	0.01
ZnS	-0.4677	-0.22	0.03	0.07	0.24	0.14	0.04
ZnSe	-0.4496	-0.23	0.01	0.06	0.18	0.12	0.03
ZnTe	-0.3925	-0.22	0	0.05	0.13	0.1	0.01
CdTe	-0.3117	-0.2	0	0.04	0.15	0.09	0.04

Figure 1: Form factors in Rydberg of the pseudopotentials of 14 band structures

The pseudopotential Hamiltonian for the crystal consists of kinetic and potential components. After evaluating all VG (pseudopotential) values, they are integrated into the Hamiltonian matrix equation:

$$H = -\frac{\hbar^2}{2m}\nabla + V(r) \tag{2}$$

Additionally, the kinetic energy is computed and incorporated into the Hamiltonian. Subsequently, the band structures for 14 materials are obtained by diagonalizing this Hamiltonian, which includes both kinetic terms and pseudopotentials.

Analyses and Results

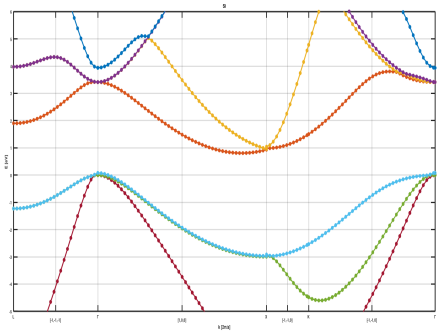

Figure 2: Band Structure of Si Computed

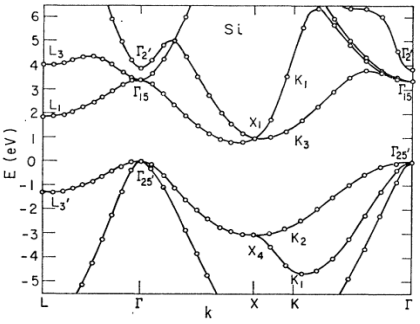

Figure 3: Band Structure of Si as in Cohen-Bergstresser

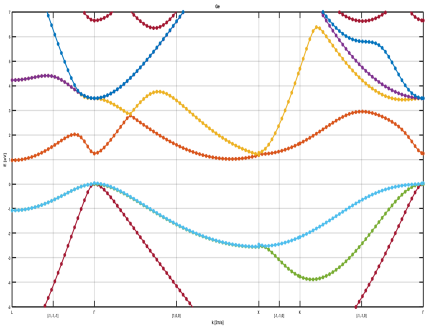

Figure 4: Band Structure of Ge Computed

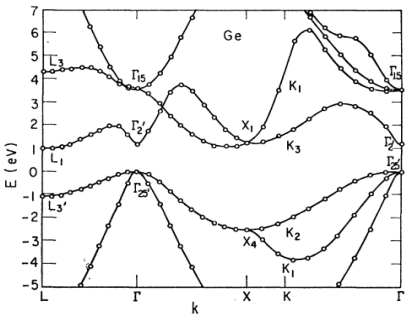

Figure 5: Band Structure of Ge as in Cohen-Bergstresser

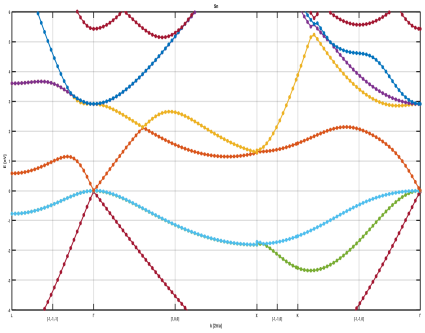

Figure 6: Band Structure of Sn Computed

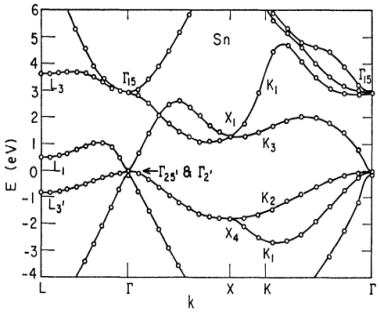

Figure 7: Band Structure of Sn as in Cohen-Bergstresser

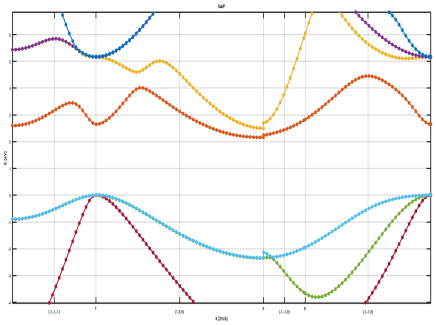

Figure 8: Band Structure of GaP Computed

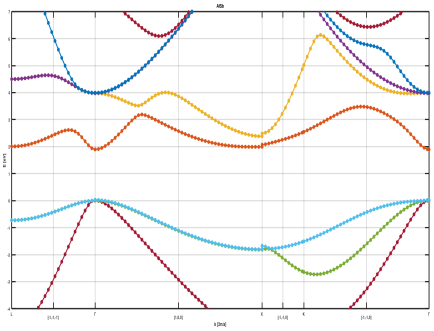

Figure 12: Band Structure of AlSb Computed

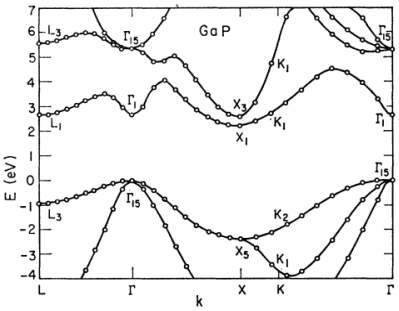

Figure 9: Band Structure of GaP as in Cohen-Bergstresser

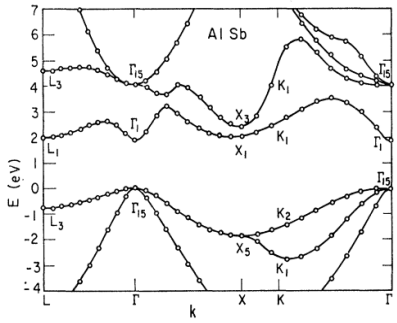

Figure 13: Band Structure of AlSb as in Cohen-Bergstresser

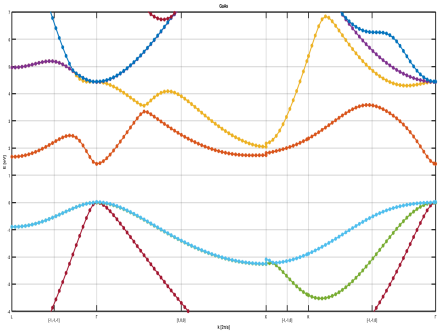

Figure 10: Band Structure of GaAs Computed

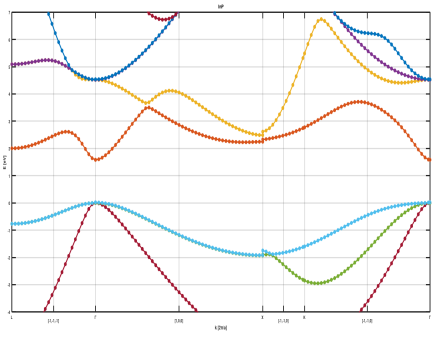

Figure 14: Band Structure of InP Computed

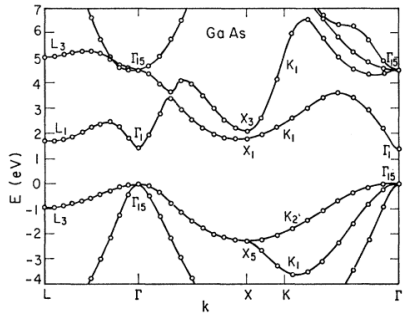

Figure 11: Band Structure of GaAs as in Cohen-Bergstresser

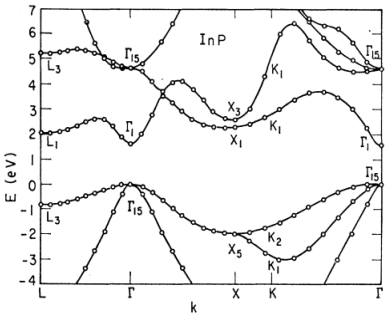

Figure 15: Band Structure of InP as in Cohen-Bergstresser

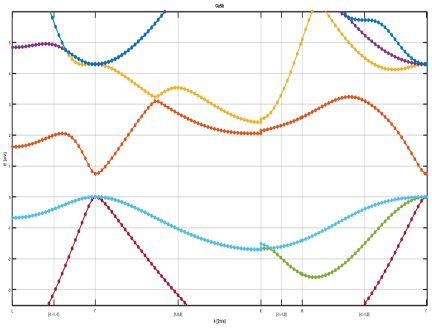

Figure 16: Band Structure of GaSb Computed

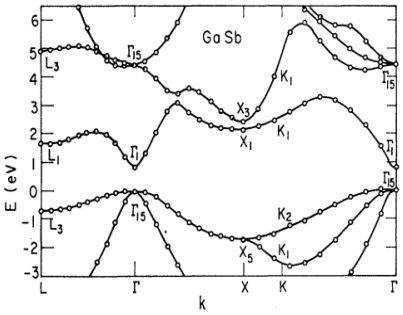

Figure 17: Band Structure of GaSb as in Cohen-Bergstresser

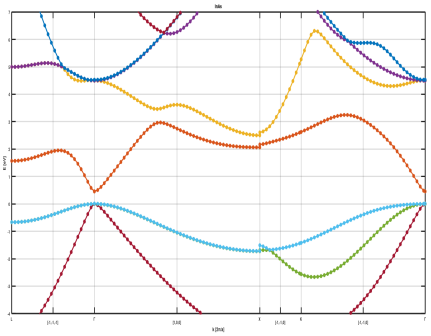

Figure 18: Band Structure of InAs Computed

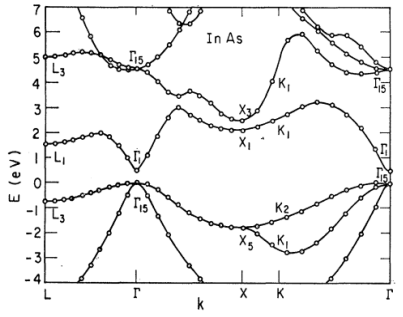

Figure 19: Band Structure of InAs as in Cohen-Bergstresser

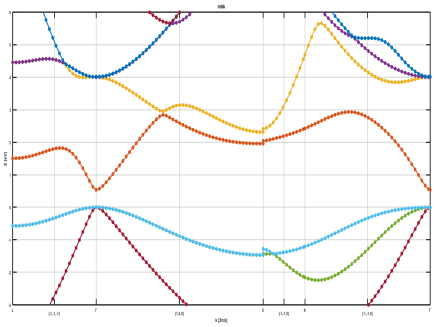

Figure 20: Band Structure of InSb Computed

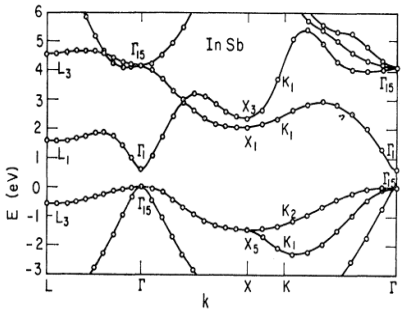

Figure 21: Band Structure of InSb as in Cohen-Bergstresser

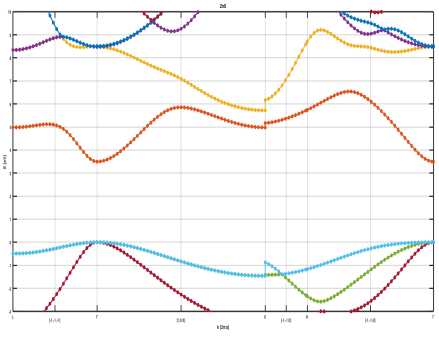

Figure 22: Band Structure of ZnS Computed

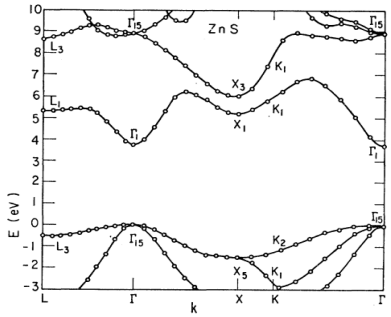

Figure 23: Band Structure of ZnS as in Cohen-Bergstresser

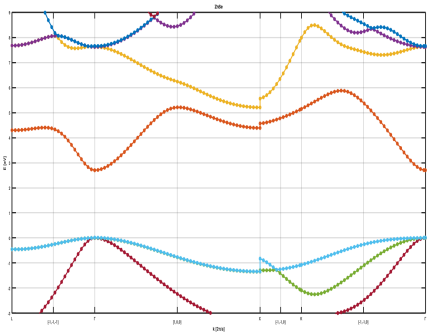

Figure 24: Band Structure of ZnSe Computed

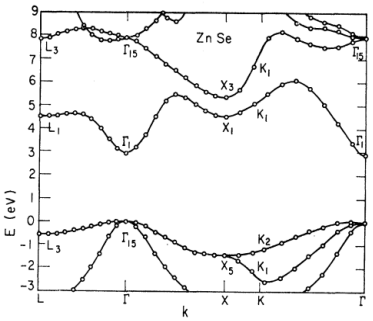

Figure 25: Band Structure of ZnSe as in Cohen-Bergstresser

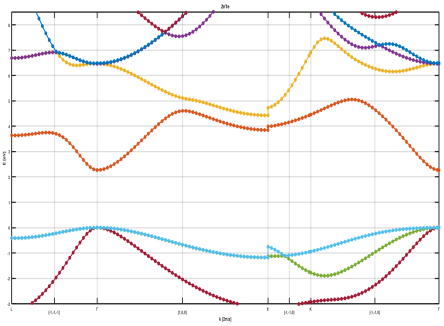

Figure 26: Band Structure of ZnTe Computed

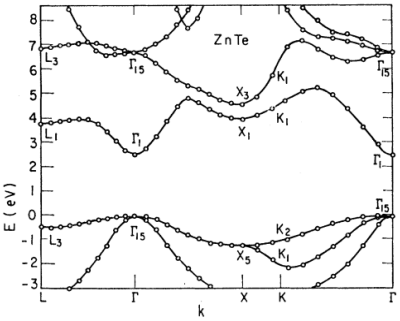

Figure 27: Band Structure of ZnTe as in Cohen-Bergstresser

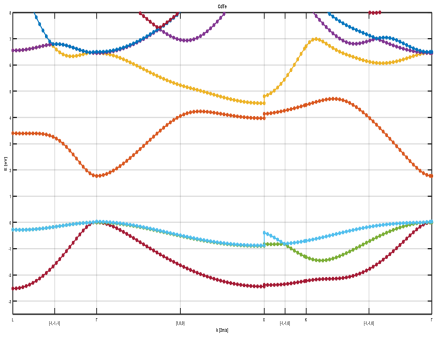

Figure 28: Band Structure of CdTe Computed

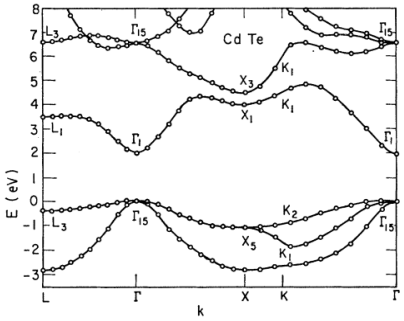

Figure 29: Band Structure of CdTe as in Cohen-Bergstresser

Analysis

In terms of feature positioning, key features like peaks, Concavity, and inflection points in the band structures align with those observed in Cohen and Bergstresser's study across the Brillouin zone. This consistency in feature positioning across all materials examined further validates the reliability of the results in comparison with the foundational research. The observed similarities in the locations of Concavities, peaks, and inflection points underscore the precision of the band structure analysis.

In the comparison of band structures, we can highlight a close resemblance of overall shapes in terms of curvature of conduction and valence bands, to the original research paper. However, we can still see some slight inaccuracies and deviations observed in Si, InAs, InSb, CdTe, and InP, particularly at specific points like X1 is "Si" with an energy of 2.6 eV compared to 2.5 eV in Cohen and Bergstresser's study. Also in Si, the second band and the fifth band increased at lower rates in the research paper than what my results showed. In addition, in ZnS, the value at X1 is around 5 ev in the researcher paper, while it is a little higher in my results(around 5.2 ev)

Regarding band gaps, we can notice a good alignment with Cohen-Bergstresser's reported values, with minor differences in several bands. In general, accurate level splitting can be seen between the Bands, however, slight deviations happen at some of the bands with around 0.1 to 0.2ev from the original paper, such as in ZnS, where the band gap between K2 and K1 is 1 ev in the paper while it is 0.1 ev smaller in my obtained results(around 0.9 ev). Some materials, such as Sn, GaSb, ZnS, and ZnSe, show identical band gap structures to the original study. However, in CdTe, the band gap between K2 at -1.2 ev and k1 at -2 ev in the research paper, is 0.2 ev lower than the value I obtained in my results(-1.2 eV for k1 and -2.2 eV for K2)

Overall, we can say that my obtained results are a good approximation to that of the research paper despite little deviations, and therefore, the computational analysis is valid and effective.

Conlcuions

In summary, the band structure analysis of 14 semiconductors closely aligns with the Cohen-Bergstresser paper. Key features such as peaks, concavity, and inflection points exhibit consistent positioning, validating the precision of the analysis. While overall shapes resemble the original research, minor variations suggest the need for nuanced consideration.

Regarding band gaps, a general alignment with the original values is observed, with slight discrepancies. Accurate level splitting between bands is maintained, emphasizing the reliability of the computational analysis. These findings support the validity and effectiveness of the study, contributing valuable insights into semiconductor electronic properties.

References

1) Cohen, M. L., Bergstresser, T. K. (1966). Band Structures and Pseudopotential Form Factors for Fourteen Semiconductors of the Diamond and Zinc-blende Structures. Phys. Rev., 141(2), 789–796. https://link.aps.org/doi/10.1103/PhysRev.141.789